Stability and internal stresses in Au(001)/Ni multilayers

Stability and internal stresses in Au(001)/Ni multilayers

Thierry Deutsch and Frédéric Lançon

Département de Recherche Fondamentale sur la Matière Condensée, SP2M, CEA, 17, rue des Martyrs, F-38054 Grenoble Cedex 9, France

Abstract
Defining the stability criteria for biaxially strained Ni, we show that the body-centred tetragonal (bct) Ni structure is not stable on an Au(001) substrate and changes to a face centred cubic (fcc) (110) structure with many stacking faults. Nevertheless, for a thin film, the bct Ni structure can be stabilized by the interface stresses. Using the stress at atomic level, the profile of the internal stresses is given as a function of Ni film thickness.

(Some figures in this article are in colour only in the electronic version)

1. Introduction

In a previous study [1, 2], we have shown that the crystalline structure of a Ni film changes as a function of its thickness when it is stacked along the (001) direction between two Au layers. The nickel is a face-centred cubic (fcc) crystal while:

- for a thickness less than 5 monolayers, the Ni layer is body-centred tetragonal (bct) close to a body-centred cubic (bcc) structure;
- for a thickness more than 5 monolayers, the Ni layer is hexagonal or 4H (ABAC stacking) with many stacking faults. The close-packed planes are perpendicular to the interfaces. This structure tends to become (110) fcc for larger thicknesses.

Our numerical simulations were in agreement with experimental results obtained by x-ray diffraction or high resolution electron microscopy. Despite a large misfit between Au and Ni lattice parameters (15.6%), no interface dislocations were found in experiments, even for large Ni thicknesses.

This paper completes our study using a potential derived from a tight-binding second moment approximation (TB-SMA). As in the previous paper [1], we restrict our study to the case of abrupt interfaces, i.e. with no mixing between Au and Ni.

First, we neglect the influence of interfaces and we analyse the stability of the bulk Ni submitted to a biaxial stress due to the Au(001) substrate. According to the dynamic theory

of crystal lattices from Born and Huang [3, 4], a crystal of N atoms can be subjected to two kinds of distortions:

- $3N - 3$ internal distortions, that can be described by all the normal coordinates q_λ of the lattice;
- 6 external distortions, that can be considered as the elements of the macroscopic homogeneous strain tensor $\boldsymbol{\eta}$.

The properties of these distortions are described, respectively, by the dynamic matrix $\mathcal{D}$ and the matrix $\mathcal{B}$, called the stiffness matrix or stress–strain matrix.

The crystal is stable with respect to all internal and external distortions if all the eigenvalues, ω_λ^2 (i.e. phonon modes), of the dynamic matrix $\mathcal{D}$ and all the eigenvalues, $\mathcal{M}_r$ ($r = 1, \ldots, 6$), of the elastic stiffness matrix $\mathcal{B}$ are positive [5, 6]. Two basic phase transitions can occur associated, respectively, with the vanishing of a phonon mode ω_λ (soft mode transition) or an eigenvalue $\mathcal{M}_r$ of the $\mathcal{B}$ matrix. In this last case, a 'spontaneous' macroscopic distortion occurs, defined by an eigenvector $\mathcal{L}_r$ which is a linear combination of the homogeneous strains η_I.

In this paper, the eigenvalues $\mathcal{M}_r$ of the elastic stiffness matrix $\mathcal{B}$ are studied to give the stability criteria for the Ni film which is commensurate with the Au(001) substrate and is subjected to an external biaxial strain of 15.6% due to the mismatch in lattice parameters. We will show that a commensurate bct Ni film on a Au(001) substrate is not stable.

After having determined the stability domain of the strained bct Ni films, our second goal is to study the influence of the Au interfaces on the Ni layer, which is more complex than a mere biaxial stress. We will describe the atomic stress distribution in the Ni exerted by the Au(001) film.

Stresses are well defined for a macroscopic solid. The global stresses are the first derivatives of the energy as a function of the strains applied on the system. On the other hand, their definition is more subtle for part of a system, such as a monolayer or even an atom. In 1970, Basinski et al [7, 8] defined a stress tensor at atomic level to study the dislocation core with a pair potential. Vitek and Egami [9–11] gave a generalized definition of a local stress tensor that can be calculated for particles interacting through a N-body potential at finite temperature.

However, this definition has a serious drawback: a chain of atoms of different types at zero pressure should have no stress located in any part of the chain, because there is no geometrical constraint to hinder a strained part of the system to expand. Indeed, in one dimension any stressed part can shrink or expand to release its stress independently of the rest of the system. The stress definition from Vitek et al does not give a zero value in this case. The same is true for a stress σ_{zz} perpendicular to a free surface that must be zero.

A rigorous but intuitive definition has been given by Lutsko [12] and permits the calculation of the stresses for any volume inside a system. Nevertheless, to our knowledge, this approach has never been used. We will give a new expression of the Lutsko definition of the stresses for any volume up to the atomic level. Then we will calculate the internal stresses for each monolayer of the Au/Ni multilayer and will show their variations as a function of the thickness of the Ni layer.

Thus, the plan of this paper is the following. In the first section, after describing briefly the form of our potential, we define the different elastic quantities which interest us: Lagrangian strains, global and atomic level stresses and the elastic stiffness matrix $\mathcal{B}$.

In the second section, we study the stability of bulk Ni subjected to a biaxial strain perpendicular to the (001) direction by calculating the stiffness matrix $\mathcal{B}$. Finally, we study the internal stresses of Au/Ni multilayers giving their profile with respect to multilayer thickness and show how a Au interface fixes a few Ni monolayers in the bct structure.

2. Definitions

2.1. Interatomic potential

We use a semi-empirical potential derived from the TB-SMA (see [1] for more details). The total potential energy is expressed as

$$E = \sum_{\{i,j\}} A_{ij} \exp\left\{-p_{ij}\left(\frac{r^{ij}}{r_0}-1\right)\right\} - \sum_i \left[\sum_j \beta_{ij}^2 \exp\left\{-2q_{ij}\left(\frac{r^{ij}}{r_0}-1\right)\right\}\right]^{1/2} \quad (1)$$

where r_0 is the nearest-neighbour distance, r^{ij} is the distance between atom i and j and A_{ij}, p_{ij}, β_{ij} and q_{ij} are four parameters depending on the nature of the atoms i and j. The sum $\sum_{\{i,j\}}$ is over all pairs $\{i, j\}$, $i < j$. This interatomic potential belongs to the more general form of the embedding atom method:

$$E = \sum_i \left[\sum_j \tfrac{1}{2}\Phi(r^{ij}) + F(\rho_i)\right] \quad (2)$$

where $\Phi(r^{ij})$ is a pair function and $F(\rho_i)$ is a function of a local electronic density ρ_i which is also expressed as a sum of a pair function $V(r_{ij})$. Note that this interatomic potential depends only on the distance between atoms: there is no angular dependence.

2.2. Lagrangian deformations

Under applied stresses, solids change their form and their volume. We define the initial position of a point of the solid by r^0 (with components r_1^0, r_2^0, r_3^0) and its final position by r. Let us use the superscript ^{0} for all quantities of the initial configuration. Therefore a symbol with superscript ^{0} is a constant with respect of any deformation, i.e. its derivatives are zero.

A deformation is homogeneous if it is uniform throughout the solid and can be defined by the nine independent parameters $u_{\alpha\beta}$, the gradients of a displacement vector u from $\{r^0\}$ to $\{r\}$. We form a tensor u with elements $u_{\alpha\beta}$ given by

$$u = r - r^0 \quad (3)$$
$$u_{\alpha\beta} = \partial u_\alpha/\partial r_\beta. \quad (4)$$

To consider finite strains, we use the Lagrangian tensor of strain η with elements

$$\eta_{\alpha\beta} = \frac{1}{2}\left(\frac{\partial u_\alpha}{\partial r_\beta} + \frac{\partial u_\beta}{\partial r_\alpha} + \sum_\gamma \frac{\partial u_\gamma}{\partial r_\alpha}\frac{\partial u_\gamma}{\partial r_\beta}\right). \quad (5)$$

For a rigid rotation, η is zero and, as it is symmetric ($\eta_{\alpha\beta} = \eta_{\beta\alpha}$), we use the Voigt notation defined by

$$\eta_1 = \eta_{11}, \qquad \eta_2 = \eta_{22}, \qquad \eta_3 = \eta_{33}$$
$$\eta_4 = 2\eta_{23}, \qquad \eta_5 = 2\eta_{13}, \qquad \eta_6 = 2\eta_{12}.$$

The energy E can be written as

$$E(\{r\}) = E(\{r^0\}, \eta) \quad (6)$$

where the Lagrangian strain tensor η describes the variation of lengths in the solid submitted to a homogeneous deformation. We have a simple relation between r and r^0:

$$r^2 - (r^0)^2 = 2\sum_{\alpha\beta} r_\alpha^0 \eta_{\alpha\beta} r_\beta^0. \quad (7)$$

Relation (7) shows that the derivative of r^2 with respect to $\boldsymbol{\eta}$ does not depend on the final value $\boldsymbol{r}$, but only on the initial value $\boldsymbol{r}^0$. Therefore $\partial r^2/\partial \eta_{\alpha\beta} = 2r_\alpha^0 r_\beta^0$ and thus

$$\frac{\partial r}{\partial \eta_{\alpha\beta}} = \frac{\partial r}{\partial \eta_I} = \frac{r_\alpha^0 r_\beta^0}{r} \tag{8}$$

where I is $(\alpha\beta)$. This relation is used to calculate the second derivatives of r as a function of η_I in the elastic constant calculation:

$$\frac{\partial^2 r}{\partial \eta_I \partial \eta_J} = r_\alpha^0 r_\beta^0 \frac{\partial (1/r)}{\partial \eta_J} = -\frac{r_\alpha^0 r_\beta^0 r_\gamma^0 r_\delta^0}{r^3}. \tag{9}$$

We point out that the vector $\boldsymbol{u}$ is not assumed to be infinitesimal; these expressions are exact for finite homogeneous strains.

2.3. Elastic constants

The elastic constants of order n are defined as the nth derivatives of the energy with respect to η_I:

$$C_{IJ...} = \frac{1}{\mathcal{V}} \frac{\partial^n E}{\partial \eta_I \partial \eta_J \ldots} \tag{10}$$

where E is the energy and V is the volume of the system. We restrict our discussion to the zero-temperature case; therefore, E is the potential energy, and not the free energy. The first-order elastic constants are the components σ_I of the stress tensor and the second-order ones are the elastic moduli C_{IJ} with $I = (\alpha\beta)$ and $J = (\gamma\delta)$. Thus, near the equilibrium, the energy E can be expanded as

$$E = E_0 + \mathcal{V} \left[\sum_I^6 \sigma_I \eta_I + \tfrac{1}{2} \sum_{I,J}^6 C_{IJ} \eta_I \eta_J + \cdots \right]. \tag{11}$$

As Martin [13, 14] has shown, this expansion of the energy as a function of η_I is only valid at zero strain for a centrosymmetric crystal (where each atom is a centre of symmetry). Otherwise, we need to take the internal elastic constants into account. The first derivative of the energy is written as

$$\frac{\partial E}{\partial r^{ij}} = \Phi'(r^{ij}) + [F'(\rho_i) + F'(\rho_j)]V'(r^{ij}) \tag{12}$$

From this equation and (2), the global stress σ_I becomes

$$\sigma_I = \frac{1}{\mathcal{V}} \sum_{\{i,j\}} \left[\Phi'(r^{ij}) + \frac{1}{2}\left(\frac{1}{\rho_i} + \frac{1}{\rho_j}\right)V'(r^{ij}) \right] \frac{r_\alpha^{ij} r_\beta^{ij}}{r^{ij}}. \tag{13}$$

In order to calculate the elastic constants from equation (10), we take the second derivatives of the potential energy. Knowing that r^{ij} depends only on r_0^{ij}, we have

$$C_{IJ} = \frac{1}{\mathcal{V}} \sum_{\{i,j\}} \left[\sum_{\{k,l\}} \frac{\partial^2 E}{\partial r^{ij} \partial r^{kl}} \frac{\partial r^{ij}}{\partial \eta_I} \frac{\partial r^{kl}}{\partial \eta_J} + \frac{\partial E}{\partial r^{ij}} \frac{\partial^2 r^{ij}}{\partial \eta_I \partial \eta_J} \right]. \tag{14}$$

Now we can write the expression of elastic constants as a function of the first and second derivatives of the energy E using (8) and (9):

$$C_{IJ} = \frac{1}{\mathcal{V}} \sum_{\{i,j\}} \sum_{\{k,l\}} \left[\frac{\partial^2 E}{\partial r^{ij} \partial r^{kl}} - \delta_{\{i,j\},\{k,l\}} \frac{1}{r^{ij}} \frac{\partial E}{\partial r^{ij}} \right] \frac{r_\alpha^{ij} r_\beta^{ij} r_\gamma^{kl} r_\delta^{kl}}{r^{ij} r^{kl}} \tag{15}$$

where $\delta_{\{i,j\},\{k,l\}}$ is a Kronecker symbol which is equal to 1 when the pairs $\{i,j\}$ and $\{k,l\}$ are identical. With respect to our interatomic potential, the second derivatives of E are

$$\frac{\partial^2 E}{\partial r^{ij} \partial r^{kl}} = \delta_{\{i,j\},\{k,l\}}[\Phi''(r^{ij}) + \{F'(\rho_i) + F'(\rho_j)\}V''(r^{ij})]$$
$$+ [(\delta_{i,k} + \delta_{i,l})F''(\rho_i) + (\delta_{j,k} + \delta_{j,l})F''(\rho_j)]V'(r^{ij})V'(r^{kl}). \tag{16}$$

From expression (10) of C_{IJ}, we can write

$$C_{IJ} = \frac{1}{\mathcal{V}} \sum_{\{i,j\}} \sum_{\{k,l\}} \left\{ \delta_{\{i,j\},\{k,l\}} \left[\Phi''(r^{ij}) - \frac{1}{r^{ij}}\Phi'(r^{ij}) \right. \right.$$
$$+ \left. (F'(\rho_i) + F'(\rho_j))\left(V''(r^{ij}) - \frac{1}{r^{ij}}V'(r^{ij}) \right) \right]$$
$$+ \left. [(\delta_{i,k} + \delta_{i,l})F''(\rho_i) + (\delta_{j,k} + \delta_{j,l})F''(\rho_j)]V'(r^{ij})V'(r^{kl}) \right\} \frac{r_\alpha^{ij} r_\beta^{ij} r_\gamma^{kl} r_\delta^{kl}}{r^{ij} r^{kl}}. \tag{17}$$

These expressions will be useful to define stability criteria.

2.4. Stresses

The global stresses being the first derivatives of E with respect to η_I, we get from equation (12) and (13)

$$\sigma_I = \frac{1}{\mathcal{V}} \sum_{\{i,j\}} \frac{\partial E}{\partial r^{ij}} \frac{r_\alpha^{ij} r_\beta^{ij}}{r^{ij}}. \tag{18}$$

For an unconstrained system in equilibrium, the stress tensor σ is zero, otherwise the system would spontaneously distort. In order to define a local stress quantity, we introduce the partial force F^{ij} which the atom j exerts on atom i as

$$F^{ij} = -\nabla_{r^{ij}} E = -\frac{\partial E}{\partial r^{ij}} \frac{r^{ij}}{r^{ij}}. \tag{19}$$

Thus, expression (18) can be written as

$$\sigma_{\alpha\beta} = -\frac{1}{\mathcal{V}} \sum_{\{i,j\}} F_\alpha^{ij} r_\beta^{ij}. \tag{20}$$

A physical interpretation of this expression can be given as follows: when we apply a deformation $\eta_{\alpha\beta}$, the distance r^{ij} changes by $r_\beta^{ij}\eta_{\alpha\beta}$ in the direction x_α. The partial force F^{ij} should oppose this displacement and does work $F_\alpha^{ij} r_\beta^{ij}\eta_{\alpha\beta}$. Then, summing over all pairs of atoms, the change of energy is

$$\Delta E = -\sum_{(\alpha\beta)} \sum_{\{i,j\}} F_\alpha^{ij} r_\beta^{ij} \eta_{\alpha\beta} \tag{21}$$

which should be equal to the first term of the expansion (11), i.e. $\mathcal{V}\sigma_{\alpha\beta}\eta_{\alpha\beta}$.

As a stress is defined in terms of the variation of energy of a certain volume, a local stress has to be associated with a given volume. More precisely, if we want to calculate the stress on a part of a system (a monolayer or an atom), we have to define, the volume $\mathcal{V}$ of this part. Then we can extend the same argument we have developed for the total solid for this volume $\mathcal{V}$.

When a strain $\eta_{\alpha\beta}$ is applied to the volume $\mathcal{V}$, the fraction p^{ij} of the distance r^{ij} included in the volume $\mathcal{V}$ changes by $p^{ij} r_\beta^{ij}\eta_{\alpha\beta}$ in the direction x_α. The force F^{ij} opposes this displacement and thus does the work $-F_\alpha^{ij} p^{ij} r_\beta^{ij}\eta_{\alpha\beta}$.

Summing over all pairs whose fraction p^{ij} varies, the energy variation due to the strain $\eta_{\alpha\beta}$ applied on the volume $\mathcal{V}$ is

$$\Delta E = -\sum_{(\alpha\beta)} \sum_{\{i,j\}} p^{ij} F_\alpha^{ij} r_\beta^{ij} \eta_{\alpha\beta}. \tag{22}$$

The local stress $\sigma_{\alpha\beta}(\mathcal{V})$ we want to introduce should verify

$$\Delta E = \mathcal{V} \sum_{(\alpha\beta)} \sigma_{\alpha\beta}(\mathcal{V})\eta_{\alpha\beta}. \tag{23}$$

Thus the stress $\sigma_{\alpha\beta}(\mathcal{V})$ of the volume $\mathcal{V}$ is defined as

$$\sigma_{\alpha\beta}(\mathcal{V}) = -\frac{1}{\mathcal{V}} \sum_{\{i,j\}} F_\alpha^{ij} p^{ij} r_\beta^{ij} \tag{24}$$

where p^{ij} is the fraction of the length of the bond $\{i, j\}$ included in the volume $\mathcal{V}$. Three kinds of intersections between a bond and a convex volume exist:

 (i) bonds completely included in the volume between two atoms inside the volume;
 (ii) bonds between an atom in the volume and another one outside;
(iii) bonds between two atoms outside the volume.

Thus the algorithm to compute the internal stress at atomic level is the following:

 (i) We choose to associate with each atom a domain corresponding to its Voronoï cell. The Voronoï cell decomposition [15] is a unambiguous way to partition space and to assign a reasonable volume to each atomic position. Other possibilities exist to define precisely an atomic volume [16]. In this paper, we will group together the individual atomic volumes to form layer volumes and compute their stresses. Using another partition should give qualitatively the same results.
 (ii) The intersections are calculated between each atomic volume and all bonds of the system.
(iii) The partial forces between atoms are calculated and finally the local stress tensor σ_i for each atom i is computed using equation (24).

Using this algorithm, for Au/Ni multilayers for instance, we are able to calculate the layer and the interfacial stresses by summing the individual atomic contributions of each monolayer.

2.5. Elastic stiffness matrix $\mathcal{B}$

To be stable, a crystal should satisfy some stability criteria. For a cubic crystal the three stability criteria [17] are

$$C_{11} + 2C_{12} > 0, \qquad C_{44} > 0, \qquad C_{11} - C_{12} > 0. \tag{25}$$

The first relation corresponds to the bulk modulus $B = (C_{11}+2C_{12})/3$ and the second and third ones correspond to shear constants, but these three criteria are only valid for an unstressed cubic system. Wallace [5, 18] has generalized these conditions for non-zero stresses by defining the coefficients of stiffness $\mathcal{B}_{IJ}$.

Let us take a crystal that is already constrained at the configuration X_0. If a strain $\eta_{\gamma\delta}$ is added to this crystal, its configuration changes from X_0 to X. The elastic stiffness matrix $\mathcal{B}$ is defined by

$$\mathcal{B}_{\alpha\beta\gamma\delta}(X_0) \equiv \left[\frac{\partial \sigma_{\alpha\beta}(X)}{\partial \eta_{\gamma\delta}}\right]_{X_0}. \tag{26}$$
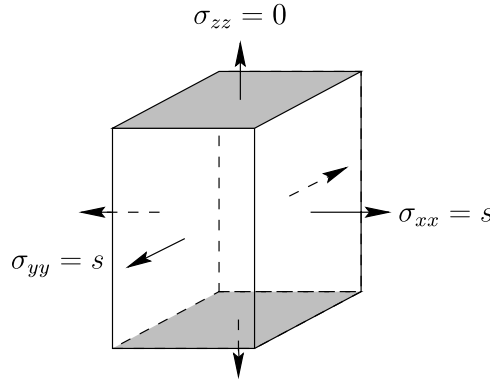
Figure 1. Tetragonal cell of Ni showing symmetries of the system and the components of the stress tensor σ.

$\mathcal{B}$ represents the second derivatives of the enthalpy. Therefore the system is stable if the matrix $\mathcal{B}$ is positive definite, i.e. all its eigenvalues are positive. The expression for $\mathcal{B}$ [5] is then

$$B_{\alpha\beta\gamma\delta} = C_{\alpha\beta\gamma\delta} + \tfrac{1}{2}[\sigma_{\alpha\delta}(\boldsymbol{X_0})\delta_{\beta,\gamma} + \sigma_{\beta\delta}(\boldsymbol{X_0})\delta_{\alpha,\gamma}$$
$$+ \sigma_{\alpha\gamma}(\boldsymbol{X_0})\delta_{\beta,\delta} + \sigma_{\beta\gamma}(\boldsymbol{X_0})\delta_{\alpha,\delta} - 2\sigma_{\alpha\beta}(\boldsymbol{X_0})\delta_{\gamma,\delta}] \tag{27}$$

where $C_{\alpha\beta\gamma\delta}$ are elastic constant coefficients defined by

$$C_{\alpha\beta\gamma\delta} \equiv \left[\frac{1}{V(\boldsymbol{X})} \frac{\partial^2 E(\boldsymbol{X})}{\partial \eta_{\alpha\beta} \partial \eta_{\gamma\delta}} \right]_{\boldsymbol{X_0}}. \tag{28}$$

Equation (27) shows that $\mathcal{B}$ depends explicitly on the stresses of the crystal at configuration $\boldsymbol{X_0}$, which is equal to the external stresses. In the general case, $\mathcal{B}$ has a different symmetry than the C symmetry. At zero stress, the elastic stiffness matrix $\mathcal{B}$ is identical to the elastic constant matrix C.

3. Stability criteria of biaxially strained fcc Ni

Now, we apply the calculation of $\mathcal{B}$ for a biaxially strained fcc Ni structure.

For a biaxial strain along the x and y axes, the stress tensor σ (see figure 1) is given by

$$\sigma = \begin{pmatrix} s & 0 & 0 \\ 0 & s & 0 \\ 0 & 0 & 0 \end{pmatrix}. \tag{29}$$

In this case, a strained fcc lattice can be described as a face-centred tetragonal (fct) lattice with the same axis system although the corresponding Bravais lattice is actually the bct one. Our initial structure being fcc, we keep the fcc axes for the distorted structure. So, in the following calculation, we consider a fct cell of Ni, called fct Ni. Because of the fct symmetry, the non-zero elastic constants of fct Ni are

$$\begin{aligned} C_{11} &= C_{22}; & C_{33}; & \quad C_{13} \\ C_{12} &= C_{23}; & C_{44}; & \quad C_{66}. \end{aligned} \tag{30}$$

Using equations (27) and (29), the elastic stiffness matrix $\mathcal{B}$ is given by

$$\mathcal{B} = \begin{pmatrix} C_{11}+s & C_{12}-s & C_{13}-s & & & \\ C_{12}-s & C_{11}+s & C_{13}-s & & 0 & \\ C_{13} & C_{13} & C_{33} & & & \\ & & & C_{44}+\frac{1}{2}s & & \\ & 0 & & & C_{44}+\frac{1}{2}s & \\ & & & & & C_{66}+s \end{pmatrix}. \tag{31}$$

3.1. Eigenvalues of $\mathcal{B}$

The structure of the tetragonal Ni is stable if the matrix $\mathcal{B}$ is positive definite, i.e. all its eigenvalues $\mathcal{M}_r$ are positive. There are five eigenvalues, $\mathcal{M}_1$ being a double eigenvalue:

$$\begin{aligned}
\mathcal{M}_1 &= \tfrac{1}{2}(2C_{44}+s) \\
\mathcal{M}_2 &= C_{66}+s \\
\mathcal{M}_3 &= C_{11}-C_{12}+2s \\
\mathcal{M}_4 &= \tfrac{1}{2}\Bigg[C_{11}+C_{12}+C_{33} \\
&\quad -\sqrt{(C_{11}+C_{12}+C_{33})^2+4(2C_{13}{}^2-C_{11}C_{33}-C_{12}C_{33}-2C_{13}s)}\,\Bigg] \\
\mathcal{M}_5 &= \tfrac{1}{2}\Bigg[C_{11}+C_{12}+C_{33} \\
&\quad +\sqrt{(C_{11}+C_{12}+C_{33})^2+4(2C_{13}{}^2-C_{11}C_{33}-C_{12}C_{33}-2C_{13}s)}\,\Bigg]
\end{aligned} \tag{32}$$

$\mathcal{M}_4$ is positive if the second factor in the square root is negative. $\mathcal{M}_5$ is always greater than $\mathcal{M}_4$. Therefore, we can write four stability criteria obtained from $\mathcal{C}_1$ to $\mathcal{C}_4$, respectively:

$$\mathcal{C}_1: \qquad 2C_{44}+s > 0 \tag{33}$$

$$\mathcal{C}_2: \qquad C_{66}+s > 0 \tag{34}$$

$$\mathcal{C}_3: \qquad C_{11}-C_{12}+2s > 0 \tag{35}$$

$$\mathcal{C}_4: \qquad C_{33}(C_{11}+C_{12})-2C_{13}(C_{13}-s) > 0. \tag{36}$$

Note that $C_{\alpha\beta}$ are the elastic constants of the strained system and not of the initial unstrained crystal.

We now determine numerically the values where the stability criteria fail. As an application, we will apply this to the Ni/Au system where the strain applied to the Ni by the Au substrate is 15.6%. We plot, in figure 2, the values corresponding to the four stability criteria of fct Ni in tension as a function of the imposed biaxial strain up to 20%. In the range [0, 20%], two criteria can fail.

The stability criterion $\mathcal{C}_4$ (36) starts to fail at a biaxial strain of 5.74% and corresponds to the vanishing of the eigenvalue $\mathcal{M}_4$. The criterion $\mathcal{C}_2$ (34) fails at a strain of 10.65%, and corresponds to the vanishing of $\mathcal{M}_2$.

The discontinuity in the slope of $\mathcal{M}_4$ at 7.5% is due to interatomic distances reaching the cut-off radius r_c of the interatomic potential. The first and second derivatives of the potential [1] are continuous, but not the third derivative at the point r_c.

3.2. Eigenvectors of $\mathcal{B}$

Each instability corresponds to a spontaneous deformation that are given by the six eigenvectors of the matrix $\mathcal{B}$. The strain eigenvectors corresponding to the double degenerate eigenvalue $\mathcal{M}_1$
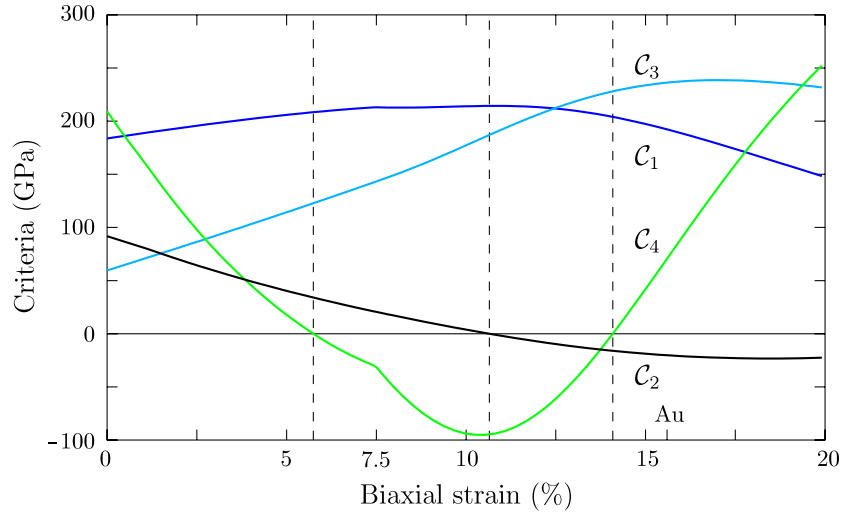
Figure 2. Curves of four stability criteria in GPa of fct Ni strained biaxially as a function of imposed strain (in per cent of linear deformation of a Ni cell).

are the η_4 and η_5 shear strains. The eigenvector $\mathcal{L}_2$ of $\mathcal{M}_2$ is the $\eta_6 = \eta_{xy}$ shear strain in the plane of subjected biaxial strain. The fourth eigenvector corresponding to $\mathcal{M}_3$ is

$$\mathcal{L}_3 = \begin{pmatrix} \eta & 0 & 0 \\ 0 & -\eta & 0 \\ 0 & 0 & 0 \end{pmatrix}. \tag{37}$$

The last two other eigenvectors are more complicated. If we define

$$\mathcal{A}_1 = \sqrt{(C_{11} + C_{12} - C_{33})^2 + 8\,C_{13}(C_{13} - s)}$$
$$\mathcal{A}_2 = (C_{12} - s)$$
$$\mathcal{A}_3 = \mathcal{A}_2(C_{33} - C_{11} - C_{12}) - 2\,C_{13}\,(C_{13} - s)$$
$$\mathcal{A}_4 = (C_{11} - 3\,C_{12} - C_{33} + 4\,s + \mathcal{A}_1)$$

and define two other quantities

$$\mathcal{U} = \frac{\mathcal{A}_3}{C_{13}\mathcal{A}_4}; \qquad \mathcal{V} = \frac{\mathcal{A}_1\mathcal{A}_2}{C_{13}\mathcal{A}_4}$$

then we can write both eigenvectors $\mathcal{L}_4$ and $\mathcal{L}_5$:

$$\mathcal{L}_{4,5} = \begin{pmatrix} \mathcal{U} \pm \mathcal{V} & 0 & 0 \\ 0 & \mathcal{U} \pm \mathcal{V} & 0 \\ 0 & 0 & 1 \end{pmatrix}. \tag{38}$$

In figure 3 are shown the two spontaneous distortions $\mathcal{L}_2$ and $\mathcal{L}_4$. The strain $\mathcal{L}_4$ preserves the tetragonal symmetry. We have two possible variants as structures: a tetragonal structure with a larger lattice constant on the z axis than the average strain, and another one with a larger lattice constant parallel to the xy plane. The strain $\mathcal{L}_2$ breaks the tetragonal symmetry and leads to four variants (see figure 3).

The tetragonal cell can be sheared along the direction x (two structures) or along the direction y (two others). This shear can lead to a fcc[011] structure. Nevertheless, the hcp, ffc[011] and 4H structures can be obtained by applying inhomogeneous shears of this type (see figure 4). The stability criteria can find the instability zones, but cannot predict what the final stable structure should be in these zones.
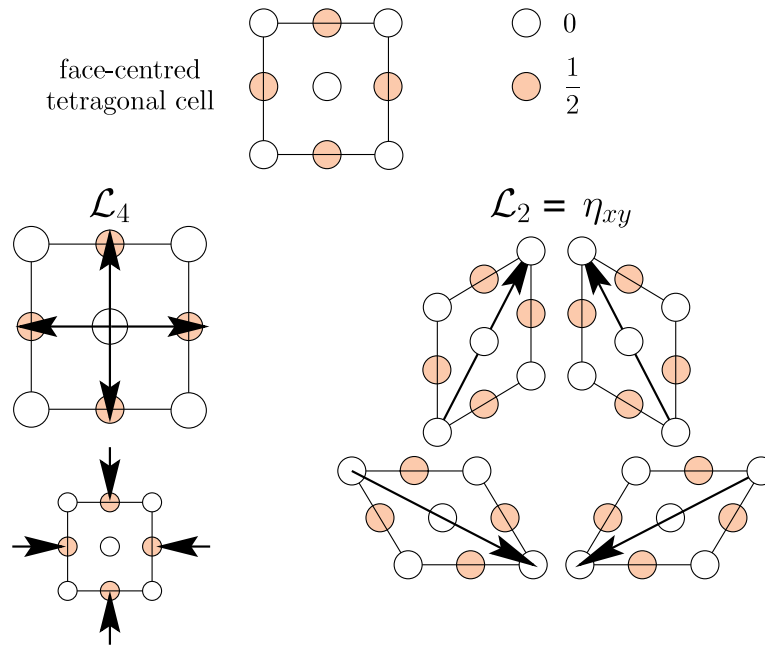
Figure 3. Strains $\mathcal{L}_4$ and $\mathcal{L}_2$ which give an unstable Ni centred tetragonal. We represent two possible structures for $\mathcal{L}_4$ and four possible structures for $\mathcal{L}_2$.
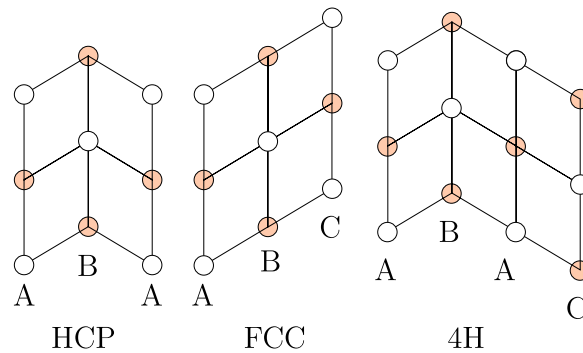

Figure 4. Hexagonal phases built from an inhomogeneous shear of (200) planes of the fct cell. The atoms denoted by grey circles are shifted by $a/2$ below or above the plane of the figure, a being the corresponding lattice constant.

3.3. Discussion

A structure is unstable along a deformation $\mathcal{L}_\epsilon$ if all forces on atoms are equal to zero but its energy is not a minimum for the strain $\mathcal{L}_\epsilon$. This structure spontaneously undergoes strain along $\mathcal{L}_\epsilon$.

From figure 2, we can distinguish four domains where the fct Ni structure is:

- stable for the domain $\mathcal{D}_1 - [0\text{–}5.74\%]$;
- unstable along the strain $\mathcal{L}_4$ for the domain $\mathcal{D}_2 - [5.74\text{–}10.65\%]$;
- unstable along the strains $\mathcal{L}_4$ and $\mathcal{L}_2$ for the domain $\mathcal{D}_3 - [10.65\text{–}14.09\%]$;
- unstable along the strain $\mathcal{L}_2$ for the domain $\mathcal{D}_4 - [14.09\text{–}\cdots]$.

These stability criteria enable the prediction of possible commensurate structure domains for Ni when it is epitaxied on a substrate that imposes a given strain.

Thus, for a strain less than 5.74% (domain $\mathcal{D}_1$), Ni stays bct, i.e. a bct nickel can grow without instability on a [001] surface of a substrate that induces a misfit less than 5.74%. Above a certain film thickness, it is obvious that dislocations or other defects will appear in order to decrease the stresses within the Ni layer, but these defects do not correspond to a spontaneous deformation of the cell.

For a deformation between 5.74 and 10.65% (domain $\mathcal{D}_2$), bct Ni is unstable along a deformation $\mathcal{L}_4$. The system prefers to create domains in which Ni relaxes towards its lattice parameter. The resulting structure is not commensurate with the substrate.

For a deformation between 10.65 and 14.09% (domain $\mathcal{D}_3$), both instabilities $\mathcal{L}_2$ and $\mathcal{L}_4$ are present.

Finally, for a deformation larger than 14.09% (domain $\mathcal{D}_4$), which is the case of Ni on an Au(001) substrate (15.6%), the Ni layer stays commensurate with the average deformation imposed by the substrate. It undergoes an inhomogeneous shear towards a hexagonal structure (see figure 3). The $\mathcal{D}_4$ domain contains Ni structures close to the unstrained fcc[011] that can be obtained with a strain of 15.8% in one direction and 21.6% in the other one. The same behaviour is predicted for Ni on Ag(001) substrate since the resulting strain is 15.77%.

To sum up, we have shown that Ni epitaxied on a fcc(001) substrate is commensurate for a strain less than 5.74% or for a strain larger than 14.09%. Then Ni adopts, respectively, a bct structure or a hexagonal structure. Between these strain values, epitaxied Ni is incommensurate with the substrate.

4. Stresses at the Au(001)/Ni interface

While defining the stability criteria in the section 3, the influence of interfaces has not been considered, i.e. we have assumed that a Ni layer between two Au films is only subjected to a uniform biaxial stress:

- $\sigma_{xx} = \sigma_{yy} = s$;
- $\sigma_{zz} = 0$;
- shear stresses σ_{xy}, σ_{xz} and σ_{yz} are equal to zero.

We have calculated the local stress tensor (equation (24)) of each monolayer in the case of Au(001)/$n \times$ Ni/Au(001) multilayers. The shear stresses $\sigma_{xy}(i)$, $\sigma_{xz}(i)$ and $\sigma_{yz}(i)$ are equal to zero for each monolayer i. The local uniaxial stresses $\sigma_{xx}(i)$, $\sigma_{yy}(i)$ and $\sigma_{zz}(i)$ vary strongly in the vicinity of Au/Ni interfaces. As expected, their average values across the film, σ_{xx} and σ_{yy}, are equal to s and the average σ_{zz} is equal to 0. In these calculations, the Au/Ni interfaces are assumed to be sharp with no mixing between Au and Ni and the Au thickness is much larger than the Ni thicknesses.

The distribution of the stress $\sigma_{zz}(i)$ has been calculated for different Ni thicknesses. Figure 5(c) shows this profile for multilayers from 2–16 Ni monolayers. The interfacial stresses extend into the two layers of Ni and Au on either side of the interface. These profiles have oscillations (a positive stress corresponds to volumes under tension and a negative stress to compression). These oscillations have the same physical origin as the oscillations of the interlayer distances at a surface or at a interface.

Figure 5(c) shows that the Au planes at the interfaces are stretched along the z axis whereas the first Ni plane is squeezed. This can be predicted with the following simple argument: the Ni layer in contact with an Au substrate is under lateral tension. Therefore it strongly contracts
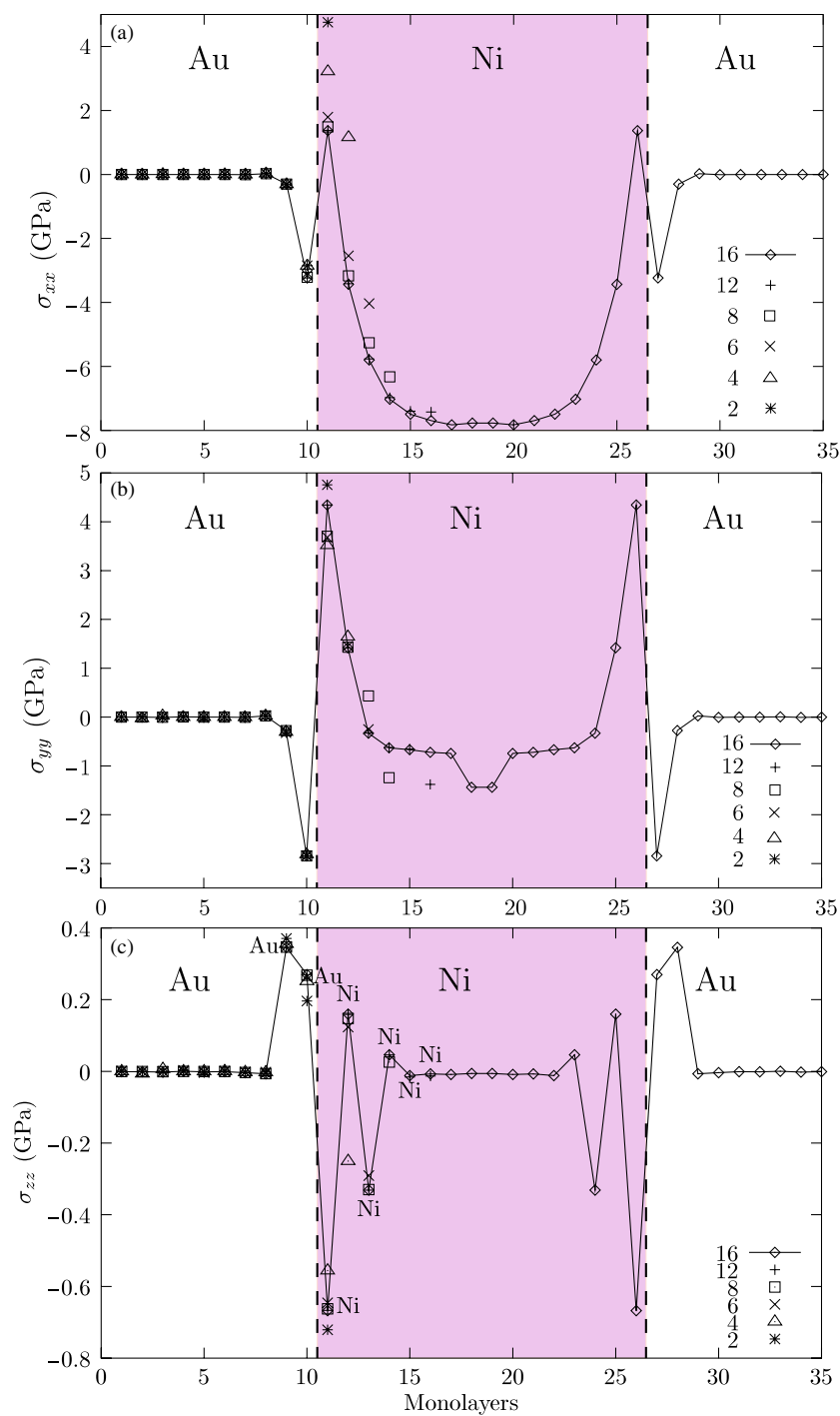
Figure 5. Curve of local stresses σ_{xx} (a), σ_{yy} (b) and σ_{zz} (c) for Au/Ni multilayers made up with 2, 4, 6, 8, 10, 12 and 16 Ni monolayers calculated for each monolayer. Ni planes are numbered from 11 to 26. Only one interface is presented except for the multilayer with 16 Ni monolayers.
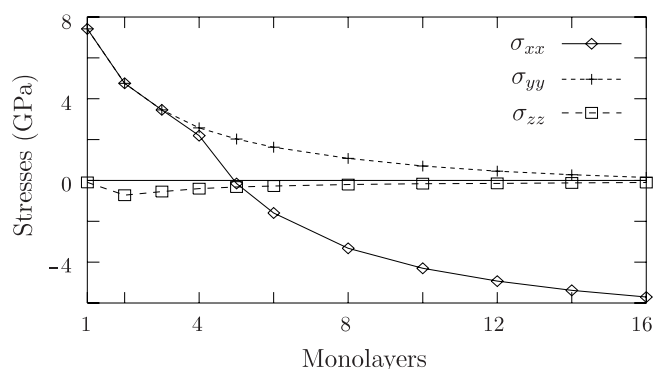
Figure 6. Curves of stresses σ_{xx}, σ_{yy} and σ_{zz} in GPa applied on a Ni layer of Au/Ni multilayers as a function of Ni thickness.

in the z direction (Poisson relation). As the average stress σ_{zz} should be equal to 0, the Au planes are under tension.

Although there are strong oscillations of $\sigma_{zz}(i)$, an important result is that the profile of stresses per monolayer across the film is mostly independent of Ni layer thickness. The profile shape is conserved even if the system undergoes a structural transition at $n = 5$.

The transition is associated with a change to the lateral stress in Ni (see figure 5): it is extended in the bct structure identically in the x and y directions and in compression mostly in the x direction in the hexagonal state. However, as for the z direction, the y profile close to the interface is not affected significantly.

At 8 Ni monolayers, the local stresses in the middle of the Ni film tend to constant values: 0 for $\sigma_{zz}(i)$, about -1 GPa for $\sigma_{yy}(i)$ and about -8 GPa for σ_{xx}. This is coherent with the fact that solids can be more easily dilated than compressed: while for the 15.6% dilation of the bct the stress is 7.42 GPa, whereas for a lower 6% compression of the hexagonal, the value is -8 GPa. Compressions give larger stress values than dilations. In figure 5(b), the dip of the stress for $\sigma_{yy}(i)$ could be the sign that twin dislocations should appear for a larger thickness in order to relax the stress.

Figure 6 gives the average stresses σ_{xx}, σ_{yy} and σ_{zz} of the whole Ni layer, i.e. the calculated stresses are averaged over all the Ni monolayers. The sign of σ_{xx} changes at five monolayers, where the structural transformation occurs. Along this direction, Ni is stretched for a thickness less than five monolayers and becomes compressed for a larger thickness. This stress could induced an enhancement of the Ni magnetic moment but the presence of non-magnetic atoms (Au) at the interface should cancel this effect [19].

5. Conclusion

In this paper, we have introduced stability criteria for a strained material. We have also given new formulae for the stresses in any volume of a solid up to the atomic level.

We have applied these criteria to predict the stability domains of Ni on fcc(001) substrates. These criteria can define commensurate growth domains of one structure on another. We have shown that, for epitaxy on Au, the pseudomorphic body-tetragonal structure is unstable with respect to a shear cell parallel to the interface. This shear gives a hexagonal structure in good agreement with experimental results [20, 21]. This general approach could be applied to other systems.

The local stresses have been introduced following Lutsko's formalism [12] and we have used them to calculate the stress profiles in Au/Ni multilayers. Applying local stresses to the interfaces or to the surfaces with terraces and kinks or interfaces would give some useful information about the elasticity at the atomic level.

Acknowledgments

References

[1] Deutsch T, Bayle P, Lançon F and Thibault J 1995 *J. Phys.: Condens. Matter* **7** 6407
[2] Deutsch T 1995 *Thèse de Doctorat* Institut National Polytechnique de Grenoble, Grenoble
[3] Born M and Huang K 1954 *Dynamical Theory of Crystal Lattices* (Oxford: Clarendon)
[4] Mirgorodsky A and Smirnov M 1994 *Ferroelectrics* **159** 139
[5] Wallace D C 1972 *Thermodynamics of Crystals* (New York: Wiley)
[6] Kim K Y 1996 *Phys. Rev.* B **54** 6245
[7] Basinski Z S, Duesbery M S, Pogany A P and Taylor R 1970 *Can. J. Phys.* **48** 1480
[8] Basinski Z S, Duesbery M S and Taylor R 1971 *Can. J. Phys.* **49** 2160
[9] Egami T, Maeda K and Vitek V 1980 *Phil. Mag.* A **41** 883
[10] Srolovitz D, Maeda K, Vitek V and Egami T 1981 *Phil. Mag.* A **44** 847
[11] Egami T and Srolovitz D 1982 *J. Phys. F: Met. Phys.* **12** 2141
[12] Lutsko J F 1988 *J. Appl. Phys.* **64** 1152
[13] Martin J W 1975 *J. Phys. C: Solid State Phys.* **8** 2837
[14] Martin J W 1975 *J. Phys. C: Solid State Phys.* **8** 2858
[15] Voronoï G 1908 *J. Reine Angew. Math.* **134** 198
[16] Gellatly B and Finney J 1982 *J. Mol. Biol.* **161** 305
[17] Wang J, Yip S, Phillpot S R and Wolf D 1993 *Phys. Rev. Lett.* **71** 4182
[18] Wallace D C 1970 *Solid State Phys.* **25** 301
[19] Ernst A, Lueders M, Temmerman W, Szotek Z and van der Laan G 2000 *J. Phys.: Condens. Matter* **12** 5599
[20] Bayle P, Deutsch T, Gilles B, Lançon F, Marty A and Thibault J 1994 *Ultramicroscopy* **56** 94
[21] Bayle P, Deutsch T, Gilles B, Lançon F, Marty A, Thibault J, Colliex C and Tence M 1994 *Defect-Interface Interactions (MRS Symp. Proc. vol 319)* ed E P Kvam, A H King, M J Mills, T D Sands and V Vitek (Pittsburg, PA: Materials Research Society)